Electronic Supplementary Material (ESI) for Physical Chemistry Chemical Physics.

Supporting information for

Temperature-dependent studies of a new two-dimensional cadmium dicyanamide framework exhibiting an unusual temperature-induced irreversible phase transition into a three-dimensional perovskite-like framework

Mirosław Mączka,[a] Anna Gągor,[a] Maciej Ptak[a], Dagmara Stefańska[a] and Adam Sieradzki[b]*

[a]*Institute of Low Temperature and Structure Research, Polish Academy of Sciences, Box 1410, 50-950 Wrocław 2, Poland*

[b]*Department of Experimental Physics, Wrocław University of Technology, Wybrzeże Wyspiańskiego 27, 50-370, Wrocław, Poland*

e-mail: m.maczka@int.pan.wroc.pl

Table S1. Selected geometric parameters (Å, º)

PhaseI			
Cd1—N1	2.314 (3)	Cd1—N4^{iv}	2.322 (3)
Cd1—N1^{ii}	2.314 (3)	Cd1—N3^{ii}	2.325 (3)
Cd1—N4^{iii}	2.322 (3)	Cd1—N3	2.325 (3)
PhaseII			
Cd1—N3	2.3115 (13)	Cd1—N5	2.3176 (13)
Cd1—N4	2.3161 (13)	Cd1—N1	2.3264 (13)
Cd1—N2	2.3149 (13)	Cd1—N6	2.3326 (14)
N8—C2^{ii}	1.304 (2)	N10—C16	1.5192 (18)
N9—C1	1.311 (2)	N10—C10	1.5189 (18)
N9—C4^{iii}	1.3102 (19)	N10—C13	1.5237 (18)
N1—C1	1.151 (2)	N10—C7	1.5210 (19)
N2—C2	1.150 (2)	C7—C8	1.517 (2)
N3—C3	1.147 (2)	C8—C9	1.521 (2)
N4—C4	1.1533 (19)	C10—C11	1.516 (2)
N5—C5	1.148 (2)	C11—C12	1.523 (2)
N6—C6	1.152 (2)	C13—C14	1.522 (2)
N7—C3	1.293 (2)	C14—C15	1.527 (2)
N7—C6^{i}	1.299 (2)	C16—C17	1.520 (2)
N8—C5	1.304 (2)	C17—C18	1.522 (2)
N3—Cd1—N4	90.59 (5)	C5—N8—C2^{ii}	119.44 (14)
N3—Cd1—N2	91.95 (5)	C1—N9—C4^{iii}	118.91 (13)
N4—Cd1—N2	94.73 (5)	N1—C1—N9	173.58 (16)
N3—Cd1—N5	89.39 (5)	N2—C2—N8^{iii}	174.00 (17)
N4—Cd1—N5	88.08 (5)	N3—C3—N7	171.94 (18)
N2—Cd1—N5	176.87 (5)	N4—C4—N9^{ii}	174.74 (16)
N3—Cd1—N1	87.06 (5)	N5—C5—N8	174.48 (17)
N4—Cd1—N1	177.40 (5)	N6—C6—N7^{iv}	172.78 (18)
N2—Cd1—N1	86.48 (5)	C16—N10—C10	108.95 (11)
N5—Cd1—N1	90.77 (5)	C16—N10—C13	110.97 (11)
N3—Cd1—N6	179.05 (5)	C10—N10—C13	107.80 (11)
N4—Cd1—N6	90.07 (5)	C16—N10—C7	108.41 (11)
N2—Cd1—N6	87.32 (5)	C10—N10—C7	111.55 (11)

N5—Cd1—N6	91.30 (5)	C13—N10—C7	109.17 (11)
N1—Cd1—N6	92.29 (5)	C8—C7—N10	115.68 (12)
C1—N1—Cd1	163.71 (13)	C9—C8—C7	109.97 (14)
C2—N2—Cd1	148.80 (13)	N10—C10—C11	115.86 (12)
C3—N3—Cd1	143.92 (13)	C10—C11—C12	109.21 (13)
C4—N4—Cd1	145.99 (13)	N10—C13—C14	115.79 (12)
C5—N5—Cd1	161.56 (14)	C15—C14—C13	109.25 (13)
C6—N6—Cd1	132.66 (13)	N10—C16—C17	116.08 (12)
C3—N7—C6^{i}	123.45 (16)	C18—C17—C16	108.78 (13)

Symmetry code(s): (i) -*x*+2, -*y*+1, -*z*+2; (ii) -*x*+3/2, *y*, -*z*+3/2; (iii) -*x*+3/2, *y*-1, -*z*+3/2; (iv) *x*, *y*-1, *z*; (v) -*x*+3/2, *y*+1/2, -*z*+3/2; (vi) -*x*+3/2, *y*-1/2, -*z*+3/2; (vii) *x*-1/2, -*y*+1/2, *z*-1/2; (viii) *x*+1/2, -*y*+1/2, *z*+1/2.

Table S2. Room-temperature IR and Raman wavenumebrs (in cm^{-1}) of powdered 2D TPrACd and suggested assignments.[a] For the comparison sake, Raman and IR wavenumbers of 3D polymorph are also presented. Modes corresponding to the dca ligand are denoted by red colour.

Raman 3D	IR 3D	Raman 2D	IR 2D	Assignment
	3068w,b			$\nu_{as}(CH_3)$
	3040vw			$\nu_{as}(CH_3)$
2997m	2995m	3005m		$\nu_{as}(CH_3)$
2977m	2978m	2987sh	2986sh	$\nu_{as}(CH_2)$
2971m	2974m	2974m	2974m	$\nu_{as}(CH_2)$
2954m		2964sh		$\nu_{as}(CH_2)$
		2957m		
2941m	2941w	2935m	2939w	$\nu_{as}(CH_2)$
2933m				$\nu_{as}(CH_2)$
2909vw	2905vw	2908w	2904vw	$\nu_{s}(CH_2)$
2879m	2885m, 2882m	2878m	2882w	$\nu_{s}(CH_3)$
			2302w	overtone
2294sh	2292m, 2286sh		2287m	$\nu_{s}(C\equiv N)$
2282w	2265vw	2281w	2264w	$\nu_{s}(C\equiv N)$
2243vs	2237m	2239vs	2234m	$\nu_{s}(C\equiv N)$
2237sh		2232m		$\nu_{s}(C\equiv N)$
2195vw	2211vw		2212vw	$\nu_{as}(C\equiv N)$
2165sh	2174s, 2166sh	2165vw	2167s	$\nu_{as}(C\equiv N)$
2156m		2150m		$\nu_{as}(C\equiv N)$
	2140sh	2121vw	2139sh	$\nu_{as}(C\equiv N)$
	1481sh			$\delta_{as}(CH_3)$
	1472m		1473m	$\delta_{as}(CH_3)$
1462sh	1462w	1462m	1461w	$\delta_{s}(CH_3)$
1454m		1450m	1455sh	$\delta_{s}(CH_3)$
1399vw		1406vw		$\omega(CH_2)$

1387vw	1384w	1382vw	1379m	$\omega(CH_2)$
1351w	1354m	1353w	1354w, 1341m	$\nu_{as}(N\text{-}C)$
1330w	1326w	1335w	1327w	$\omega(CH_2)$
1318w				$\omega(CH_2)$
1310vw		1309w		$\omega(CH_2)$
	1271vw	1289vw	1271vw	$\omega(CH_2)$
	1187vw	1184vw		$\tau(CH_2)$
1173vw	1172w	1170w	1171w	$\tau(CH_2)$
1154vw	1157vw	1151vw		δ(skeletal)
1138w	1139vw	1135w		δ(skeletal)
1104w	1104w	1101m	1100w	δ(skeletal)
1083vw				overtone
1040m	1040w	1036m	1037w	δ(C-C-C)
1030sh				δ(C-C-C)
984vw	986w	983w	984m	δ(C-N-C) + δ(C-C-C)
	969w		965m	δ(C-N-C) + δ(C-C-C)
942vw		933m	931w	δ(C-N-C)
926m	922w			$\nu_s(N\text{-}C)$
	915w	916m	916w	$\nu_s(N\text{-}C)$
872w	872vw	870w	871vw	ν(C-C)
849w	850vw	848w	848vw	δ(C-N-C)
782sh				ν(C-N-C)
773w		770w		$\rho(CH_2)$
756w	754w	757w	756sh	$\nu(NC_4) + \rho(CH_2)$

		749vw	749w	$\nu(NC_4) + \rho(CH_2)$
664m	660w	678m	675w	δ_s(N-C-N)
		645m		δ_s(N-C-N)
608vw		607w		overtone
539w		536w, 531w	531m	γ_s(N-C-N)
515w	521w	517w		δ_{as}(N-C-N)
510sh	510w	512w	510m	γ_{as}(N-C-N)
378w				$\delta(NC_4)$
362w		363w		$\delta(NC_4)$
345w		343w		δ(skeletal)
334w				δ(skeletal)
310m		309m		δ(skeletal)
245sh				T'(dca) + T'(Cd)
218m		220s		T'(dca) + T'(Cd)
196w		185w		T'(dca) + L(dca) + T'(Cd)
163s		161m		T'(dca) + L(dca) + T'(Cd)
141s		137s		T'(dca) + L(dca) + T'(Cd)

[a]Key: s, strong; m, medium; w, weak; vw, very weak; sh, shoulder; b, broad; ν, δ, γ, ω, τ, ρ, T' and L denotes stretching, in-plane bending, out-of-plane bending, wagging, twisting, rocking, translational and librational, respectively.

Table S3. Room-temperature Raman wavenumbers (in cm^{-1}) of 2D TPrACd single crystal measured in different scattering geometries corresponding to A_g and B_g Raman-active modes of

the *P*2/*n* phase.[a] Modes below 100 cm^{-1} were observed with use of the eclipse filter. Modes corresponding to the dca ligand are denoted by red colour.

c(aa)c – A_g	c(bb)c – A_g	a(cc)a – A_g	a(cb)a – B_g	a(ba)c – B_g	Assignment
3007m	3006w	3004w	3000w	3007w	$\nu_{as}(CH_3)$
		2988w	2991w	2987w	$\nu_{as}(CH_2)$
2975m	2975m	2977m	2975w	2975m	$\nu_{as}(CH_2)$
2967m				2964m	$\nu_{as}(CH_2)$
		2957m	2957m	2952w	$\nu_{as}(CH_2)$
2947sh	2947sh				$\nu_{as}(CH_2)$
2937m	2936m	2936m	2935vw	2935vw	$\nu_{as}(CH_2)$
2909w	2908w	2908w	2909vw	2909vw	$\nu_{s}(CH_2)$
2879m	2879m	2879m	2879w	2879w	$\nu_{s}(CH_3)$
			2280w		$\nu_{s}(C\equiv N)$
2239m	2239vs	2239m	2240m	2239m	$\nu_{s}(C\equiv N)$
2232m		2232m	2232m	2232w	$\nu_{s}(C\equiv N)$
	2166vw				$\nu_{as}(C\equiv N)$
2151vw	2152vw	2151vw	2151m	22150w	$\nu_{as}(C\equiv N)$
1464w	1462vw	1464w	1461sh	1461sh	$\delta_{s}(CH_3)$
1450w	1449w	1452w	1448vw	1448vw	$\delta_{s}(CH_3)$
	1404vw				$\omega(CH_2)$
	1384vw				$\omega(CH_2)$
1353vw		1354w			$\nu_{as}(N\text{-}C)$
1335w	1335w	1336w			$\omega(CH_2)$
	1310w	1309vw			$\omega(CH_2)$
			1171w	1171w	$\tau(CH_2)$
1151vw		1151vw			δ(skeletal)

1134vw	1133vw	1134vw			δ(skeletal)
1101w	1101w	1101w	1100w	1100w	δ(skeletal)
	1077vw				overtone
1036w		1037w	1036w	1036w	δ(C-C-C)
1030sh	1029w	1029w			δ(C-C-C)
			982vw	982vw	δ(C-N-C) + δ(C-C-C)
934w	934w	934w	933vw	933vw	δ(C-N-C)
913w	914vw	914vw	916w	916w	ν_s(N-C)
			872w	872w	ν(C-C)
849w		849w			δ(C-N-C)
770w	770w	770w			ρ(CH_2)
758vw		749vw			ν(NC_4) + ρ(CH_2)
677vw	670m	677w	677vw	677w	δ_s(N-C-N)
645w		645w	645w		δ_s(N-C-N)
537vw	537sh, 530w	538vw		536w	γ_s(N-C-N)
			517w		δ_{as}(N-C-N)
			509w	510w	γ_{as}(N-C-N)
	364w				δ(NC_4)
			344w	344w	δ(skeletal)
310w	310w	310w			δ(skeletal)
	220s	220w	220w	220w	T'(dca) + T'(Cd)
189w		184w			T'(dca) + L(dca) + T'(Cd)
			160w	160w	T'(dca) + L(dca) + T'(Cd)
134m	140m, 133sh	133m	134m	144m	T'(dca) + L(dca) + T'(Cd)
c(aa+ab)c –	c(bb+ba)c –	a(cc+cb)a –			

A_g+B_g	A_g+B_g	A_g+B_g	
70w	70m	70m	T'(Cd)+T'(TPrA)+L(TPrA)
	56m		T'(Cd)+T'(TPrA)+L(TPrA)
44s	49m	44s	T'(Cd)+T'(TPrA)+L(TPrA)
32m	31m		L(CdN_6)
20w	20s	20w	L(CdN_6)

[a]Key: s, strong; m, medium; w, weak; vw, very weak; sh, shoulder; b, broad; ν, δ, γ, ω, τ, ρ, T' and L denotes stretching, in-plane bending, out-of-plane bending, wagging, twisting, rocking, translational and librational, respectively.

Table S4. Raman wavenumebrs (in cm^{-1}) of 2D TPrACd single crystal measured at 400, 300 and 80 K in *c(aa+ab)c* and *c(bb+ba)c* polarization configurations.[a]

c(aa+ab)c – A_g+B_g			c(bb+ba)c – A_g+B_g			
400 K	300 K	80 K	400 K	300 K	80 K	Assignment
2298w	3006m	3016m, 3004m 3000m	2997w	3004w	3015w, 3004sh 2999w	$\nu_{as}(CH_3)$
2971m	2975m	2979m, 2973m	2972m	2974m	2973m, 2969sh	$\nu_{as}(CH_2)$
	2966w	2959w		2958vw	2961w	$\nu_{as}(CH_2)$
2939m				2947vw	2950w	$\nu_{as}(CH_2)$
2933m	2935m	2935m	2935m	2934m	2935m	$\nu_{as}(CH_2)$
2907vw	2908w	2920w, 2908m	2907vw	2907w	2908w	$\nu_{s}(CH_2)$
2879m	2879m	2888w, 2876m	2880m	2880m	2876m	$\nu_{s}(CH_3)$
	2280vw	2284w		2279vw	2284w, 2262w	$\nu_{s}(C\equiv N)$
2243vs	2239m	2244s	2236vs	2239vs	2243vs, 2232w	$\nu_{s}(C\equiv N)$
2233sh	2231sh	2232s			2222w, 2218w	$\nu_{s}(C\equiv N)$
				2164vw	2168m	$\nu_{as}(C\equiv N)$
2158m	2151m	2157m	2150w	2150w	2157m	$\nu_{as}(C\equiv N)$
	1463w	1463w		1461w	1458w	$\delta_{s}(CH_3)$
1452w	1453w	1454m	1451w	1447w	1447w	$\delta_{s}(CH_3)$
				1404vw	1405vw	$\omega(CH_2)$
				1384vw	1392vw, 1382vw	$\omega(CH_2)$
	1354w	1354w	1348vw	1349vw	1353vw	$\nu_{as}(N\text{-}C)$
	1335w	1337w	1331vw	1334w	1337w	$\omega(CH_2)$
	1310vw	1310w	1309vw	1310w	1308w	$\omega(CH_2)$
1169vw	1170vw	1174vw	1167vw	1169vw	1173w	$\tau(CH_2)$
	1152vw	1154vw			1153vw	δ(skeletal)
1138vw	1134vw	1137vw	1134vw	1133vw	1136vw	δ(skeletal)
1102w	1101w	1102w	1100w	1099w	1101w	δ(skeletal)
				1076w	1080w	overtone

1034w	1037w	1039w	1034w	1037w	1039w	δ(C-C-C)
	1030w	1032w		1029sh	1030sh	δ(C-C-C)
				984vw	989w	δ(C-N-C) + δ(C-C-C)
929w	933w	936w	927w	932w	936w	δ(C-N-C)
	915w	921w		914vw	919w	ν_s(N-C)
				899w	900w	ν(C-C)
869vw	870vw	871w	872vw	870w	871w	δ(C-N-C)
848vw	849w	851w			851vw	δ(C-N-C)
	770w	774w		769w	773w	ρ(CH_2)
758vw	757vw	755w, 749vw		746vw	748vw	ν(NC_4) + ρ(CH_2)
667m	677w	677w	664m	675m	678m	δ_s(N-C-N)
	645w	648w			647vw, 612vw	δ_s(N-C-N)
	607vw	614w		606vw	614w	overtone
535vw		555w	531vw	537sh, 529w	554vw, 538w, 528w	γ_s(N-C-N)
514vw			513vw	519vw	517vw	δ_{as}(N-C-N)
					509vw	γ_{as}(N-C-N)
362vw	370vw	374vw		364w	367w	δ(NC_4)
340w	343w	348w		343w	346w	δ(skeletal)
308w	310w	311w	309w	310w	311w	δ(skeletal)
	240w	252w, 238vw			250w	T'(dca) + T'(Cd)
		233vw				
219m	219w	222vw	218s	219s	222s	T'(dca) + T'(Cd)
		202w			200w, 190w	T'(dca) + L(dca) + T'(Cd)
		190vw, 174vw				T'(dca) + L(dca) + T'(Cd)

145s	137s	149s, 145m	142m	140m, 133sh	148m, 143sh	T'(dca) + L(dca) + T'(Cd)
		136m			135w	
		124vw, 104vw	124m		111vw	T'(dca) + L(dca) + T'(Cd)
		98vw				
	70s	80s	79w	73m	77m	T'(Cd)+T'(TPrA)+L(TPrA)
	60s	64s		56m	61m	T'(Cd)+T'(TPrA)+L(TPrA)
			48m	48m	47m	T'(Cd)+T'(TPrA)+L(TPrA)
			31m	32m	32w	$L(CdN_6)$
			14s	20s	24s	$L(CdN_6)$
					19w, 16w	$L(CdN_6)$

[a]Key: s, strong; m, medium; w, weak; vw, very weak; sh, shoulder; b, broad

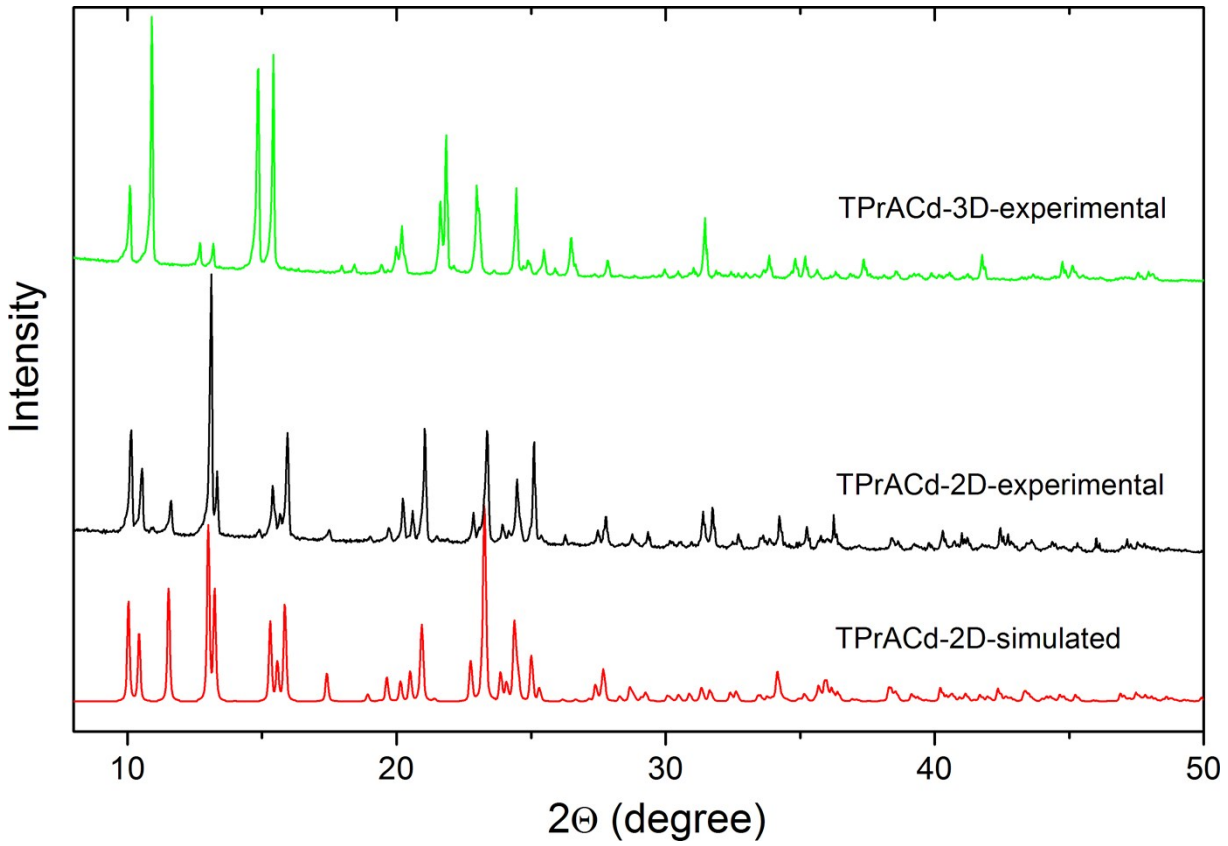

Figure S1. Room-temperature powder XRD pattern for the as-prepared 2D sample together with the calculated one based on the single crystal structures at 297 K. For the comparison sake, room-temperature XRD pattern of the 3D (perovskite) phase is also presented.

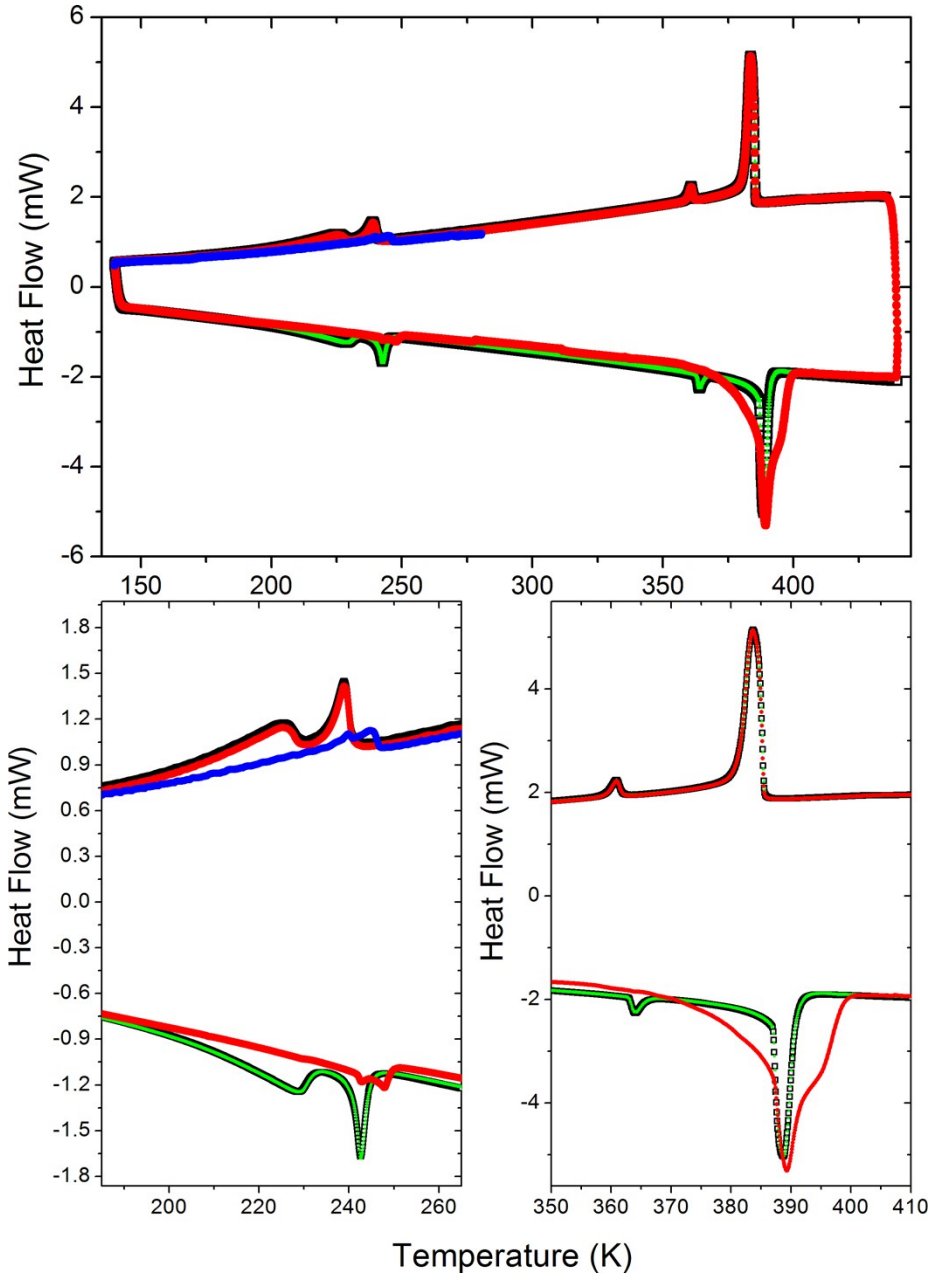

Figure S2. DSC traces for the prepared sample in heating and cooling modes: cooling from 280 to 140 K (1 cycle, blue), heating from 140 K to 440 K and cooling from 440 K to 140 K (second cycle, red), heating from 140 K to 440 K and cooling from 440 K to 270 K (third cycle, green).

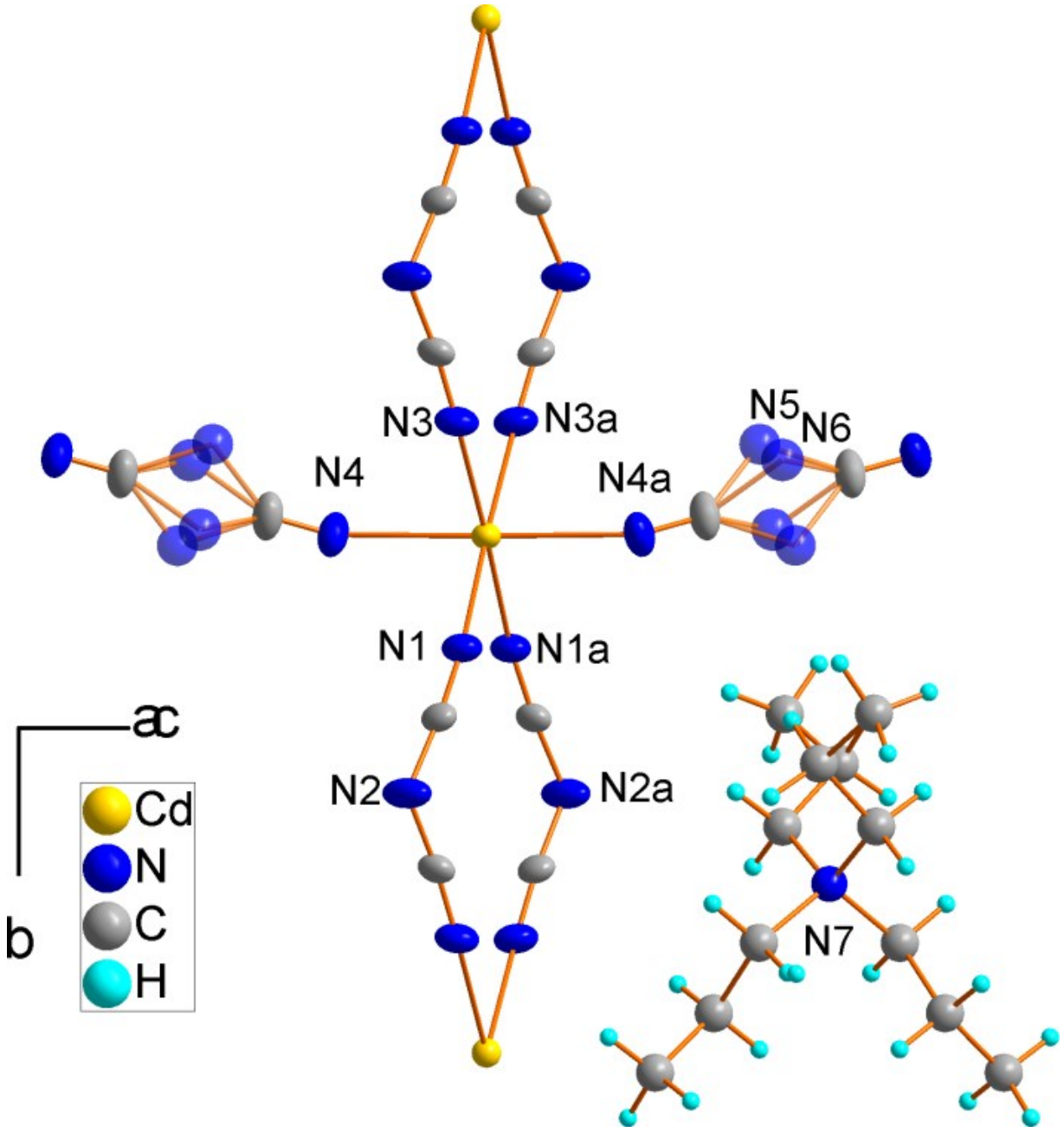

Figure S3. Coordination of cadmium atoms in the 2D phase I.

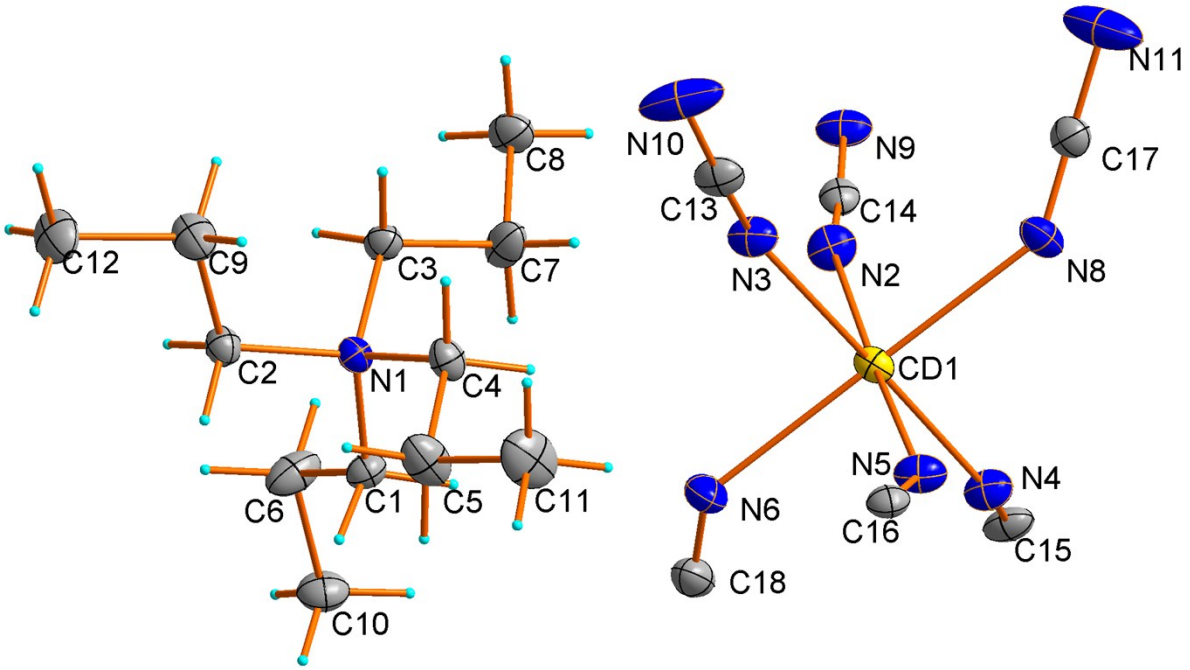

Figure S4. The content of the asymmetric unit in the low temperature phase II with the atoms numbering scheme, T=120K. Displacement elipsoids are drawn at 50% probability level.

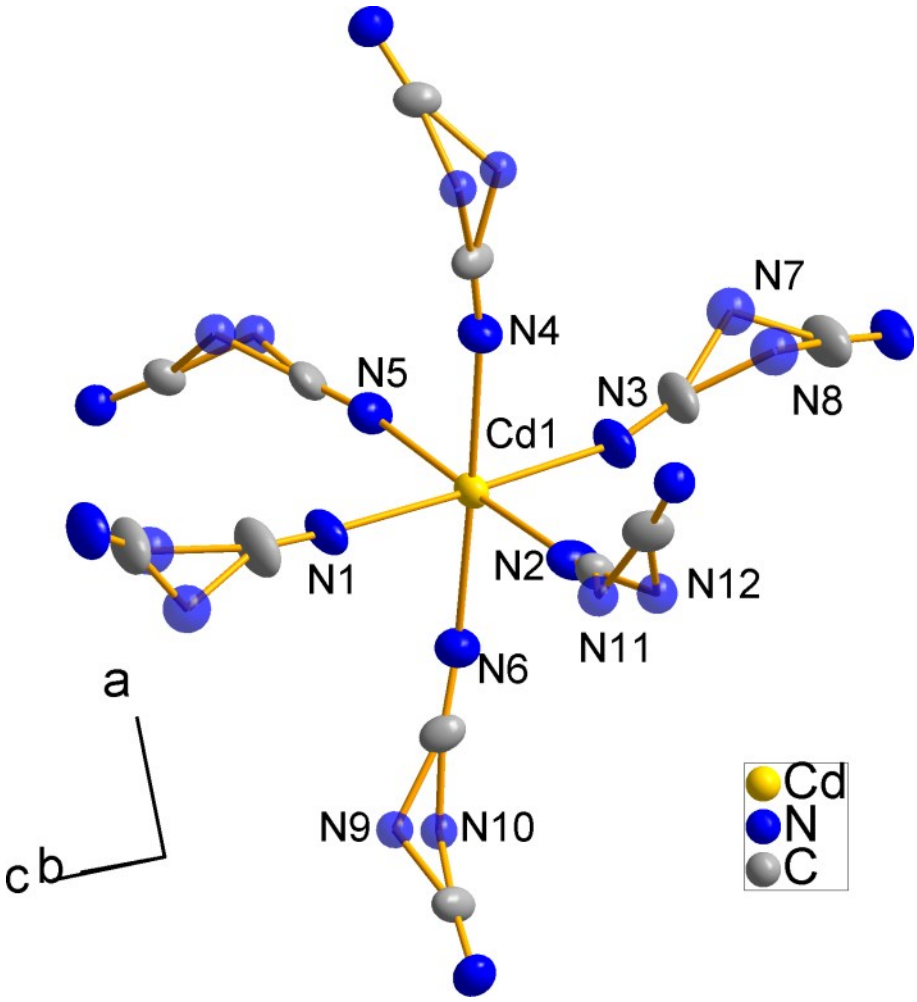

Figure S5. Coordination of cadmium atoms in the 3D phase I.

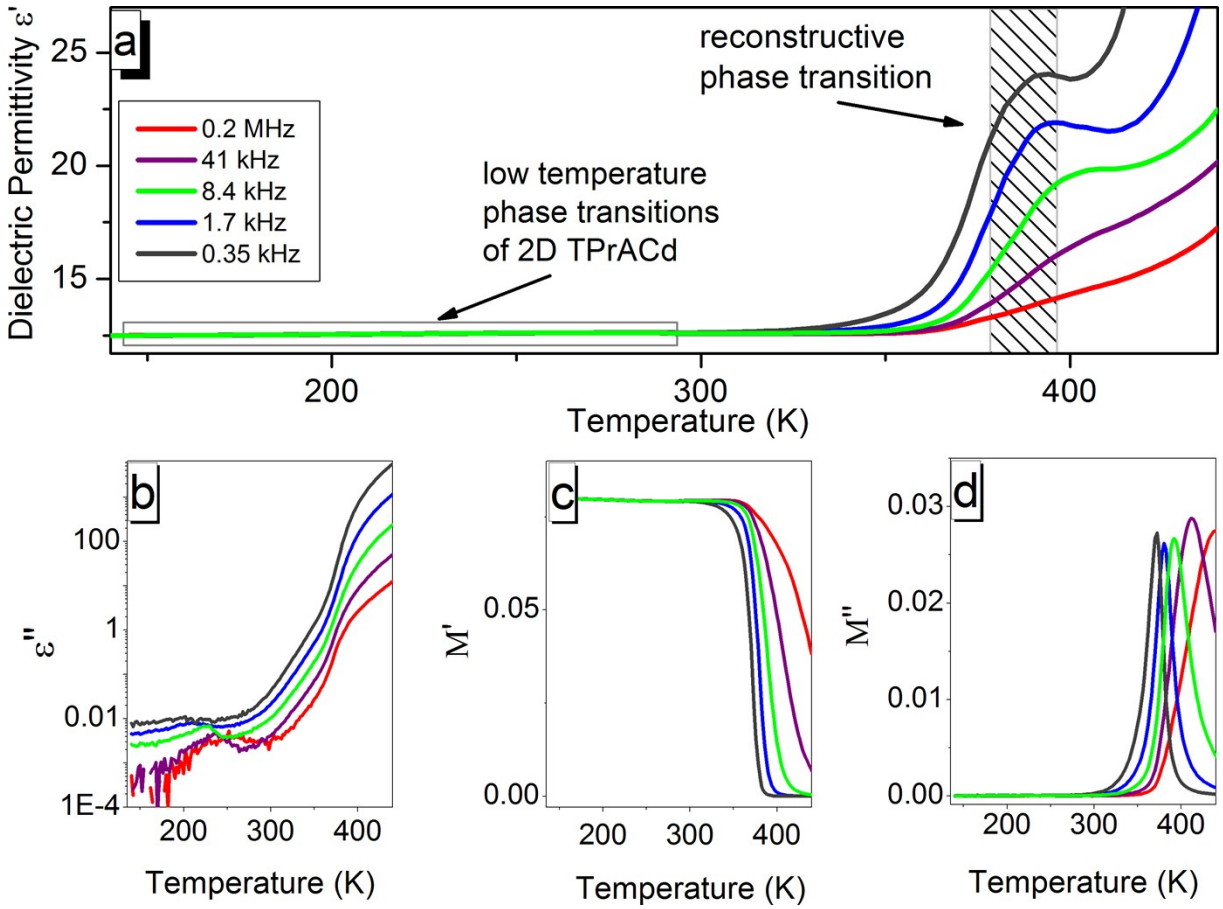

Figure S6. (a) The dielectric permittivity ε' (a) and loss (b) spectra vs temperature of 2D TPrACd at selected frequencies. The temperature dependence of real M' (c) and imaginary M" (d) pat of electric modulus. At high temperature some conductivity relaxation process is depicted.

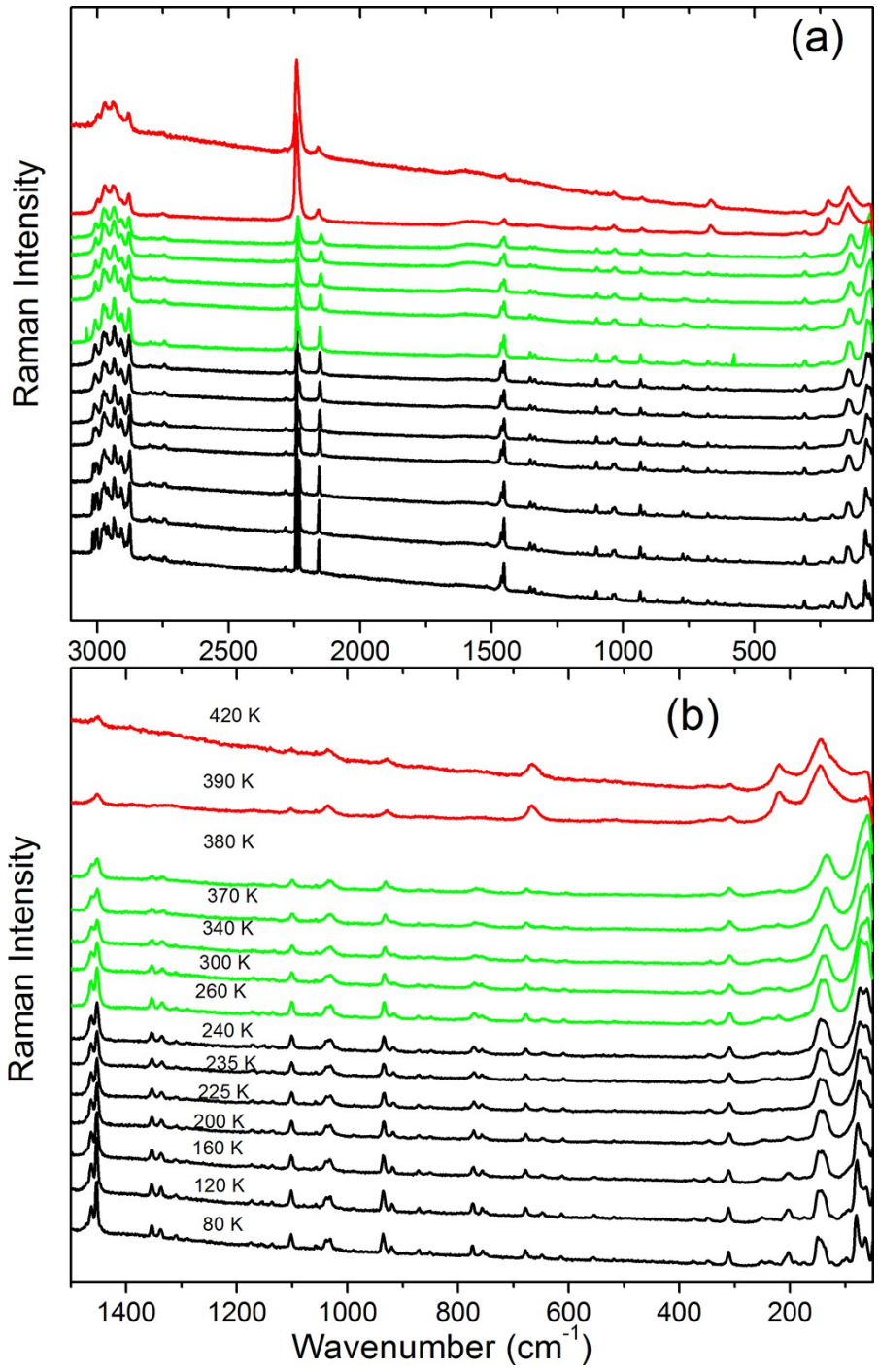

Figure S7. Temperature-dependent Raman spectra of 2D TPrACd in the whole wavenumber range corresponding to polarization c(aa+ab)c – A_g+B_g.

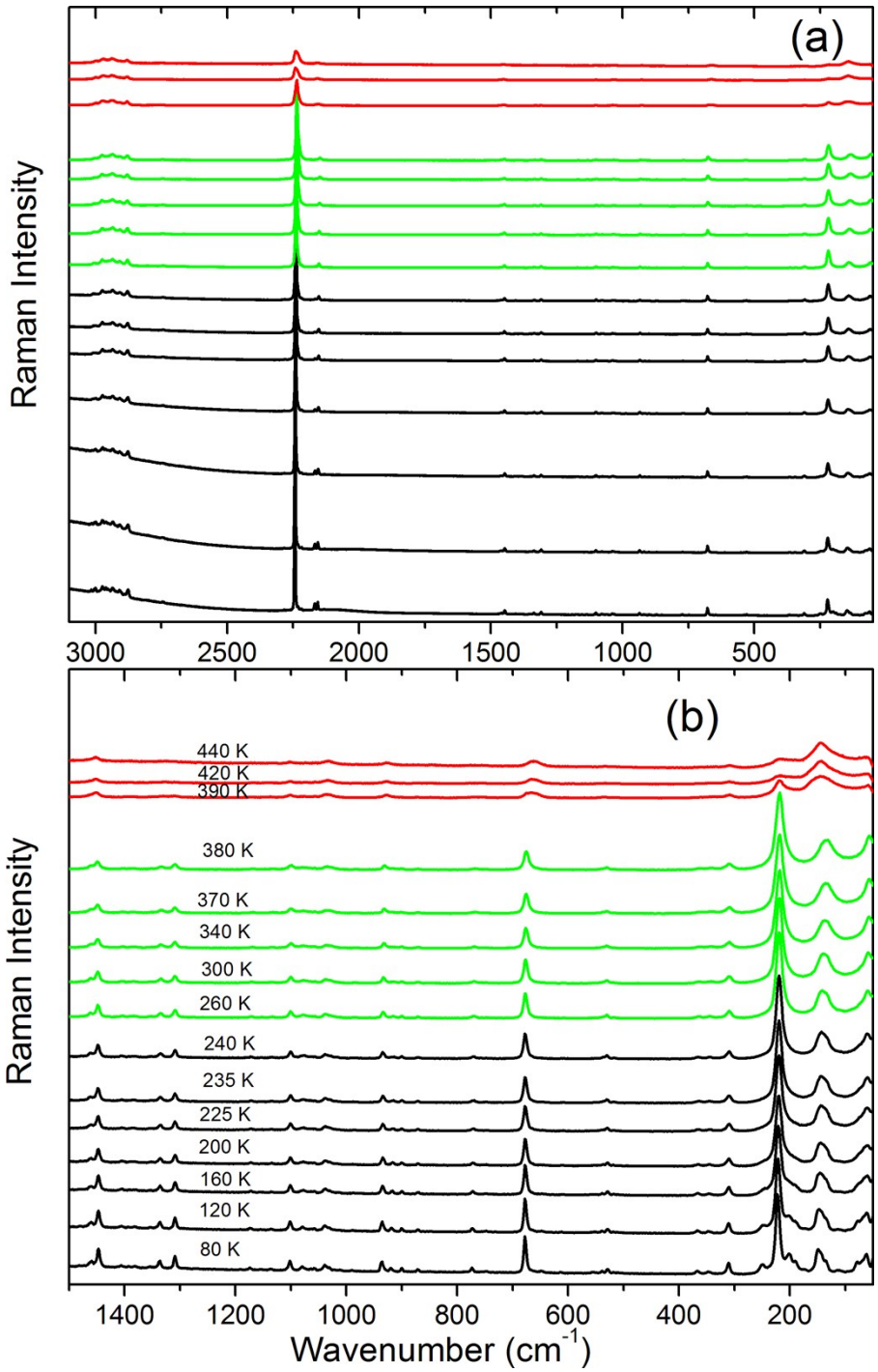

Figure S8. Temperature-dependent Raman spectra of 2D TPrACd in the whole wavenumber range corresponding to polarization c(bb+ba)c – A_g+B_g.

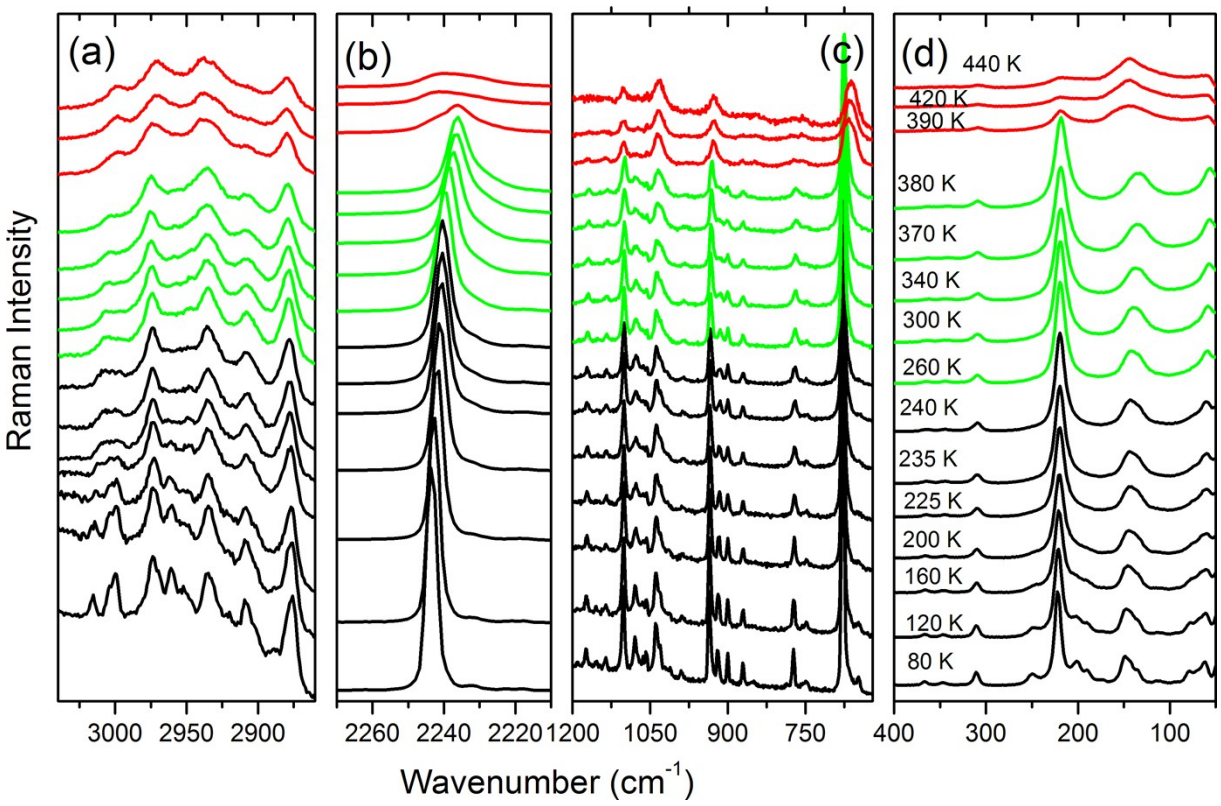

Figure S9. Details of the temperature-dependent Raman spectra of 2D TPrACd corresponding to polarization c(bb+ba)c – A_g+B_g in the spectral ranges 3040-2860, 2270-2210, 1200-720 and 400-50 cm^{-1}.Temperature-dependent Raman spectra of 2D TPrACd in the whole wavenumber range corresponding to polarization c(bb+ba)c – A_g+B_g.

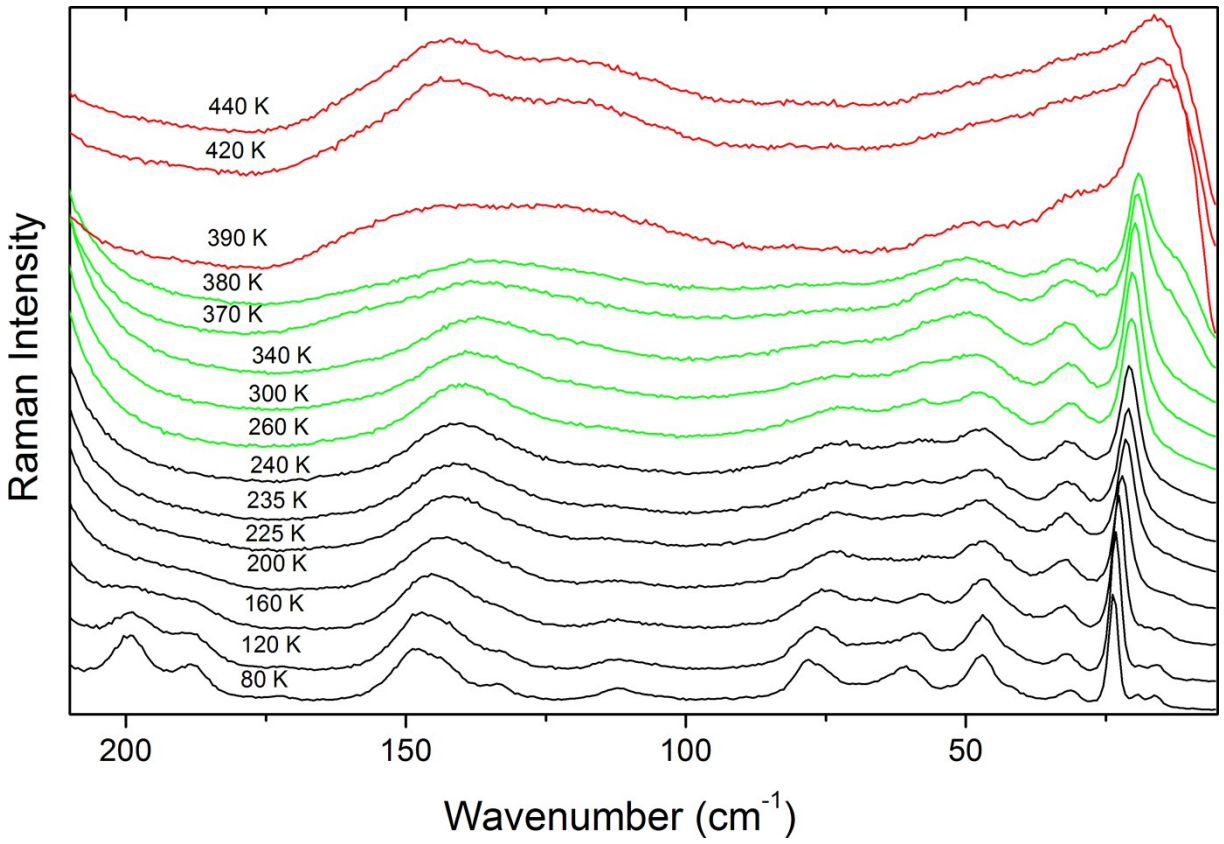

Figure S10. Temperature-dependent Raman spectra of TPrACd measured with use of the eclipse filter in polarization c(bb+ba)c – A_g+B_g.

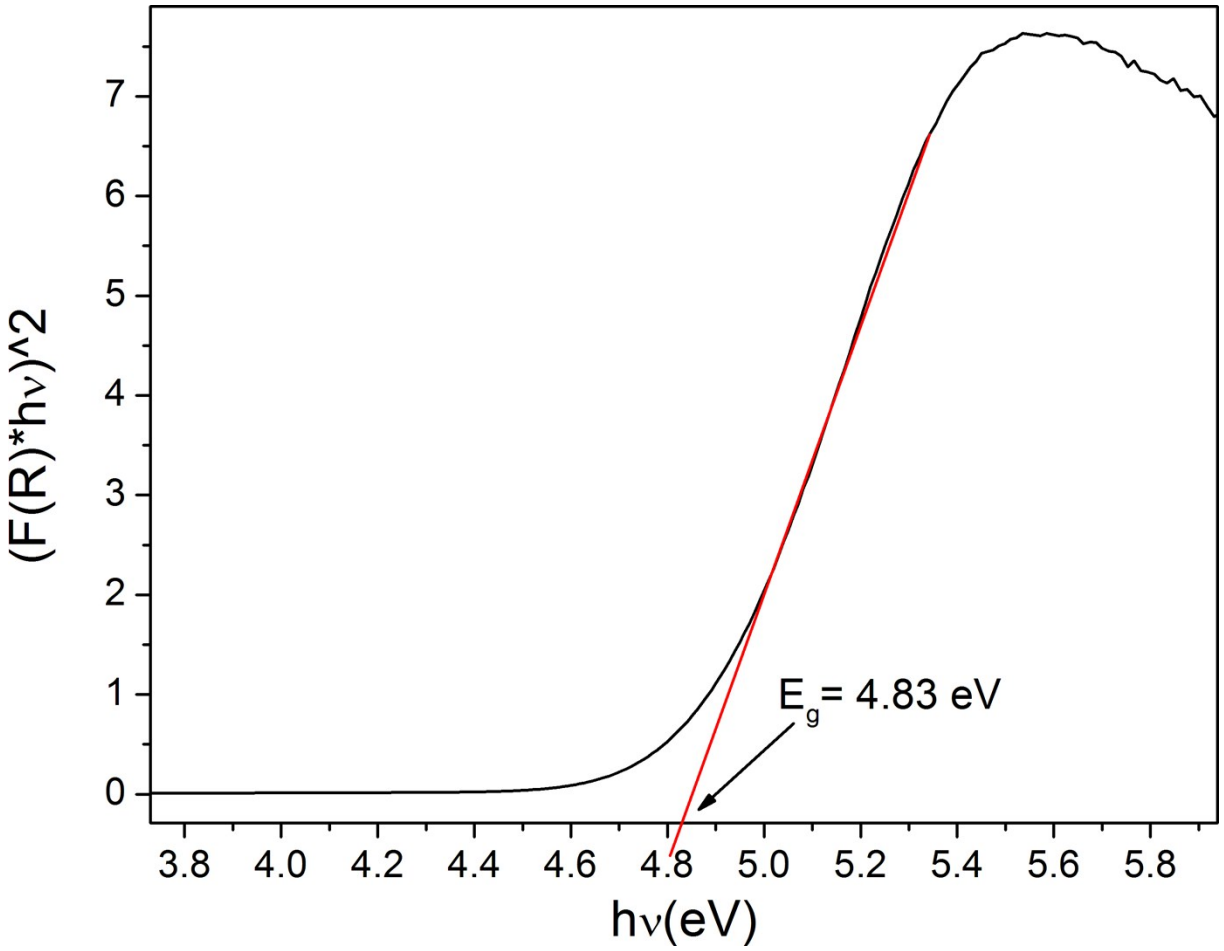

Figure S11. The determination of optical band gap of TPrACd using Kubelka – Munk function.

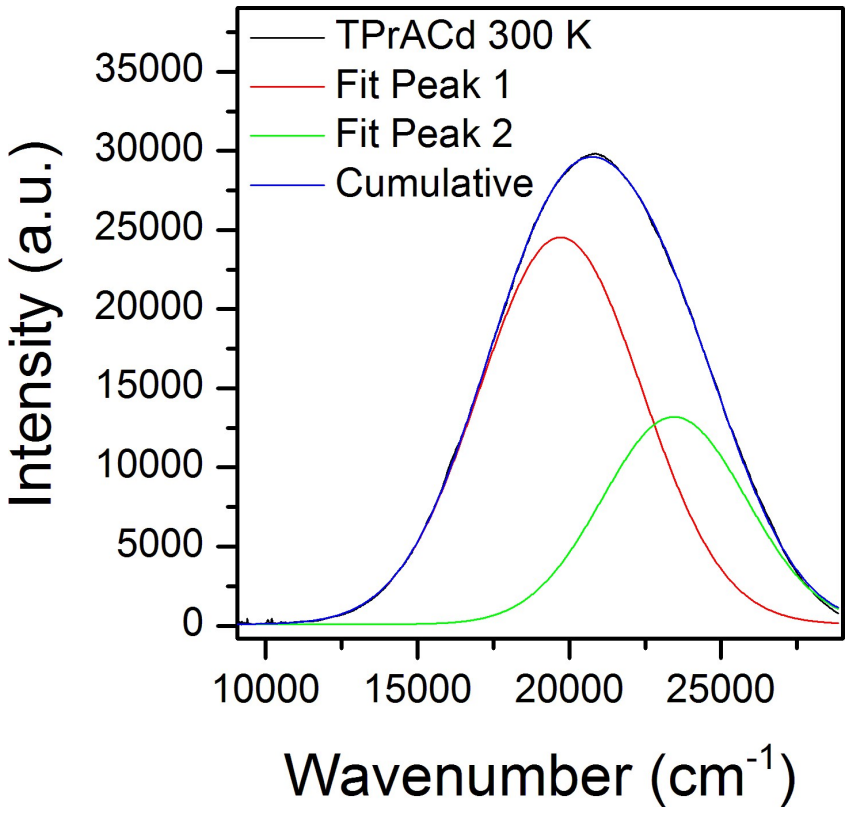

Figure S12. Deconvolution of the 300 K emission spectrum of TPrACd.

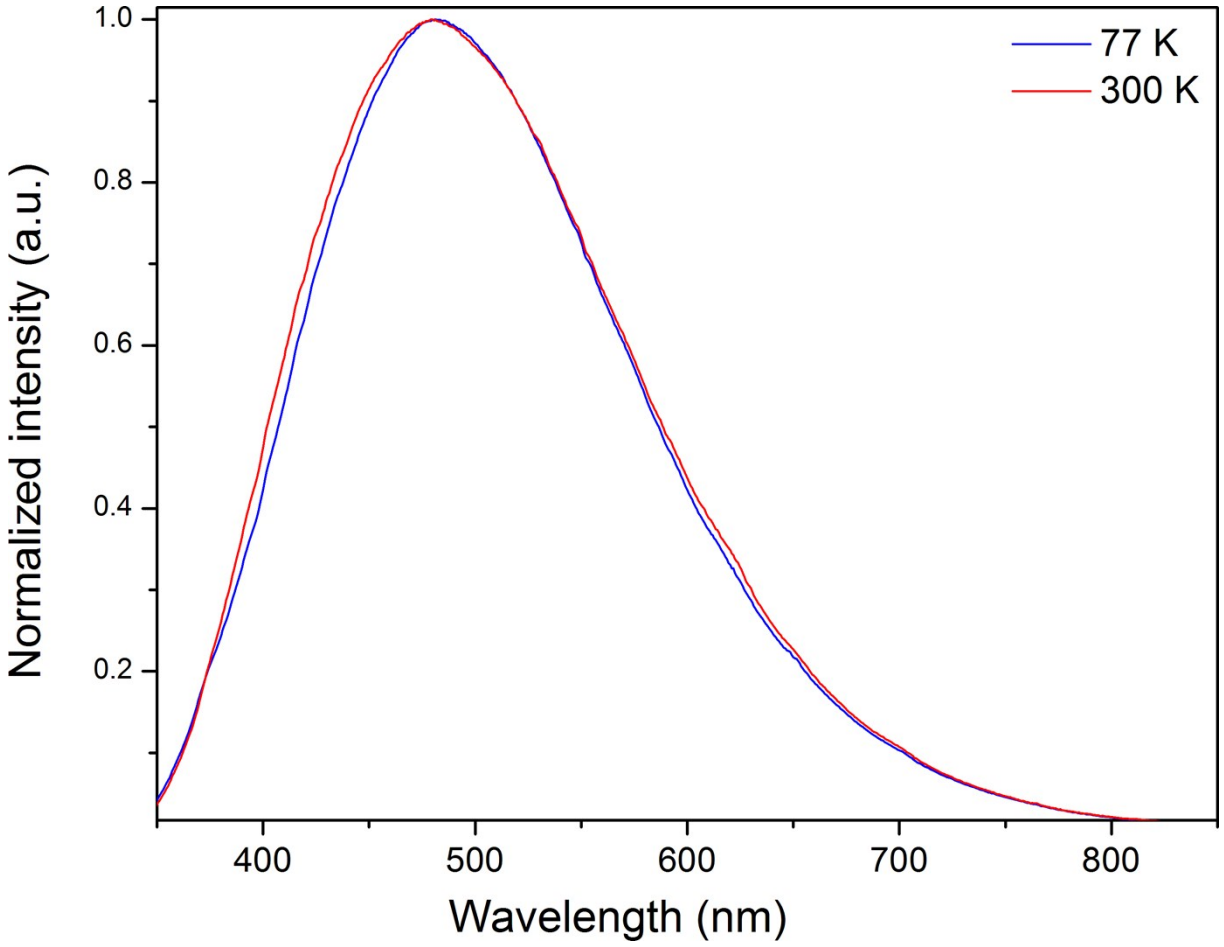

Figure S13. Normalized emission spectra of TPrACd excited at 266 nm recorded at 77 (blue line) and 300 K (red line).